



(MUDIMA)



Green Synthesis and Characterization of Ag/ZnO Nanocomposites Mediated by *Phyllanthus acidus* Leaf Extract

Mega Silvia Dewi¹, Noor Hindryawati^{2*}, Subur P. Pasaribu³

Mulawarman University

Corresponding Author: Noor Hindryawati hindryawati@gmail.com

ARTICLE INFO

Keywords: Ceremai, Ag/ZnO Nanocomposites and Characterization

Received : 2 January

Revised : 23 February

Accepted : 25 March

©2026 Dewi, Hindryawati, Pasaribu:
This is an open-access article distributed under the terms of the [Creative Commons Attribution 4.0 International](https://creativecommons.org/licenses/by/4.0/).



ABSTRACT

Ceremai leaf extract contains flavonoid and phenolic compounds that can function as reducing and capping agents. The purpose of this study was to determine the characteristics of Ag/ZnO nanocomposites synthesized with ceremai leaf extract. Ceremai leaf extract functions as a natural reducing agent. Ag/ZnO nanocomposites were made by first synthesizing silver nanoparticles, adding Zn (CH₃CO₂)₂ and NaOH until the mixture's pH reached 12. During the synthesis process, a magnetic stirrer was used to accelerate homogenization. After that, the Ag/ZnO nanocomposites were washed until the pH was neutral, then oven-dried and calcined. The resulting Ag/ZnO nanocomposite was characterized using UV-Vis Spectrophotometer, PSA, TEM, and XRD, yielding results showing that the Ag/ZnO nanocomposite was formed at λ_{\max} (nm) 370–385 nm and was stable for 6 days. The particle size distribution was bimodal, with the dominant sizes at 150, 8 nm and 671.2 nm. The morphology of ZnO as a matrix was blunt triangular and tended to be less uniform with irregular silver nanoparticles that tended to agglomerate distributed on the ZnO surface. Based on the results of the image J software, the majority of the ZnO particle size distribution was in the range of 116.52–134.87 nm. The average effective diameter \pm standard deviation of ZnO is 145.45 ± 25.95 , and the majority of the silver nanoparticle size distribution is in the range of 3.58–8.41 nm. The average effective diameter \pm standard deviation of silver nanoparticles is 7.25 ± 3.73 . ZnO has a hexagonal wurtzite structure and Ag has a face-centered cubic (FCC) structure, so ZnO is the main matrix and Ag is dispersed as nanoparticles on the surface of ZnO

INTRODUCTION

In industry, one area of research with great potential is nanotechnology [1]. Nanotechnology is a technology that manipulates atoms and molecules to create new properties that are needed [2]. The basic component is a nanoparticle, which is a particle measuring 1-100 nm [3]. Composites are formed from two or more materials with different properties [4], Nanocomposites are materials composed of a polymer matrix reinforced by nanoparticles, both organic and inorganic, with at least one dimension measuring between 10 and 100 nm [5].

Zinc oxide (ZnO) is a semiconductor with a wide band gap of approximately 3.37 eV, which limits its photocatalytic activity to only the ultraviolet (UV) region of the spectrum [6] so that under certain conditions the effectiveness of ZnO is limited [7]. The addition of Ag dopants to ZnO can increase photocatalytic and antibacterial effectiveness. This is due to the relatively wide band gap of ZnO, so that the presence of Ag⁺ ions integrated into the ZnO lattice can expand light absorption, improve electron-hole pair separation efficiency, and provide significant potential for performance improvement [8].

Based on the principles of green chemistry, the synthesis of Ag/ZnO nanocomposites can use bioreductors derived from natural extracts. Previous studies have used extracts from *Acalypha fruticosa* leaves, pineapple peel, and *Crataegus monogyna* fruit [9], [10], [11]. The basic principle of using natural extracts is to reduce Ag⁺ to Ag⁰ in the formation of silver nanoparticles [12] then the silver nanoparticles that are formed will be dispersed on the surface of ZnO [13]. Ceremai leaf extract (*Phyllanthus acidus* (L.) Skeels) also functions as a capping agent [14].

In this study, ceremai leaf extract (*Phyllanthus acidus* (L.) Skeels) was used as a natural bioreductor for the synthesis of Ag/ZnO nanocomposites because it contains phenolic compounds [15] flavonoids and alkaloids [16]. In addition, the use of ceremai leaf extract (*Phyllanthus acidus* (L.) Skeels) is also a novelty of this study, as it has never been used for the synthesis of Ag/ZnO nanocomposites before.

METHODS

The materials used in this study included ceremai leaves (*Phyllanthus acidus*), hydrochloric acid (HCl), magnesium powder (Mg), iron(III) chloride (FeCl₃), zinc acetate [Zn(CH₃COO)₂], silver nitrate (AgNO₃), sodium hydroxide (NaOH), and distilled water. All chemical reagents were of analytical grade and purchased from Sigma-Aldrich (St. Louis, MO, USA).

Sample Preparation & Phytochemical Testing of Samples

Ceremai leaves were taken from ceremai trees in the Liang Ulu area, Kota Bangun, East Kalimantan, then washed and left at room temperature to dry. Once dry, they were cut into small pieces and blended until smooth. Extraction was carried out by weighing 4 grams of ceremai leaf powder into a beaker, then adding 160 mL of distilled water and heating it using a hot plate at 40°C for 10 minutes [17]. Next, it is filtered and the filtrate is taken for the following tests:

Flavonoid Test

The flavonoid content was identified using the Shinoda test. Briefly, 2 mL of ceremai leaf extract was placed in a test tube, followed by the addition of three drops of concentrated HCl and a small amount of Mg powder. The appearance of an orange or pink color indicated the presence of flavonoids [18].

Phenolic Test

Two milliliters of ceremai leaf extract were placed in a test tube, followed by the addition of 3–4 drops of 1% iron(III) chloride (FeCl₃) solution. The formation of a brownish-black or blue-black coloration indicated the presence of phenolic compounds [18].

Synthesis of Ag/ZnO Nanocomposites Using Bioreductors from Ceremai Leaf Extract

Concentrated ceremai leaf extract was diluted using distilled water (1:10). The diluted ceremai leaf extract was placed in a 50 mL beaker, then 100 mL of 15 mM AgNO₃ (1:2) was added and stirred using a magnetic stirrer for 2 hours. Then, 100 mL of 30 mM Zn(CH₃CO₂)₂ was added to the beaker while stirring using a magnetic stirrer for 30 minutes, and

2 M NaOH was added until the pH of the mixture reached 12, then stirred again for 1.5 hours. After that, centrifuge and collect the precipitate. The precipitate obtained is washed until the pH is neutral, then oven-dried at 150°C for 2 hours and calcined at 400°C for 4 hours [19].

Characterization

The stability of the Ag/ZnO nanocomposite formed will be analyzed using a UV-Vis spectrophotometer. Measurements will be taken at wavelengths of 350–450 nm. Absorbance values will be measured continuously for 6 days, once every hour at the same time. Then characterized using a Particle Size Analyzer (PSA, SZ-100, Horiba Scientific) to determine the particle size distribution in a sample. Transmission Electron Microscopy (TEM, HITACHI HT7700, Japan) to determine the

morphology, structure, and size of a particle. X-Ray Diffraction (XRD) to determine the structure and crystal phase of a sample.

RESULTS AND DISCUSSION

Extraction and Phytochemical Testing of Ceremai Leaf Samples (*Phyllanthus acidus* (L.) Skeels)

A total of 4 grams of prepared ceremai leaf powder (*Phyllanthus acidus* (L.) Skeels) was added to 160 mL of distilled water and heated using a hot plate at 40 °C for 10 minutes. After cooling, it was filtered and the brownish ceremai leaf extract filtrate was collected. The ceremai leaf extract was then used in qualitative phytochemical testing, with the results shown in Table 1.

Table 1. Results of Phytochemical Testing of Ceremai Leaf Extract

No.	Secondary Metabolites	Results
1	Flavonoid	+
2	Phenolic	+

Description: (+) Contains Secondary Metabolite Compounds

Based on the table above, positive ceremai leaf extract contains flavonoid and phenolic secondary metabolite compounds. Thus, ceremai leaf extract can be used as a bioreductant in the synthesis of Ag/ZnO nanocomposites.

Synthesis of Ag/ZnO Nanocomposites

The synthesis process was initially carried out by diluting the ceremai leaf extract using distilled

water (1:10), then adding it to a 50 mL beaker. Next, 100 mL of 15 mM AgNO₃ (1:2) was added and stirred using a magnetic stirrer for 2 hours. The use of a magnetic stirrer in this study was intended to accelerate the homogenization of the mixture [20]. After stirring for 2 hours, silver nanoparticles were formed, indicated by a brownish color change in the solution, as shown in Figure 1.



Figure 1. Silver Nanoparticles Synthesized Using Bioreductors from Ceremai Leaf Extract

This can also be seen and proven from the results of UV-Vis spectrophotometer tests, where silver nanoparticles generally form in the range of 400–450 nm [21] so that the optimum wavelength

measurement was performed on silver nanoparticles synthesized using a bioreductor extracted from cermai leaves.

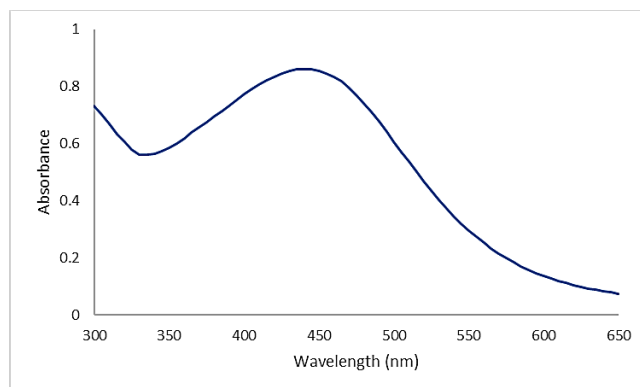


Figure 2. UV-Vis Spectrophotometer Test Results of Silver Nanoparticles Synthesized Using Ceremai Leaf Extract Bioreductant

Based on Figure 2, silver nanoparticles were formed at a wavelength of 440 nm with an absorbance of 0.861.

The silver nanoparticles formed were added to 100 mL of 15 mM $\text{Zn}(\text{CH}_3\text{CO}_2)_2$ while stirring using a magnetic stirrer for 30 minutes, resulting in a brownish solution. The addition of $\text{Zn}(\text{CH}_3\text{CO}_2)_2$ as a ZnO precursor in the formation of Ag/ZnO nanocomposites, where when ZnO interacts with Ag, its photocatalytic activity will increase due to increased electron-hole separation and decreased charge recombination. In addition, the Surface Plasmon Resonance (SPR) effect on silver nanoparticles extends absorption to the visible region (380–750 nm), thereby improving photocatalytic performance under visible irradiation [22]. After that, 2 M NaOH was added until the pH of the mixture reached 12, then stirred again using a

magnetic stirrer for 1.5 hours, resulting in a solution that changed color from brown to gray. The addition of NaOH in this study was to provide OH^- ions for Zn^{2+} ions in $\text{Zn}(\text{CH}_3\text{CO}_2)_2$. The mixture obtained was centrifuged and the precipitate was collected. The precipitate obtained was washed until the pH was neutral, then oven-dried at 150°C for 2 hours and calcined at 400°C for 4 hours to obtain a black Ag/ZnO nanocomposite.

UV-Vis Spectrophotometric Analysis of Ag/ZnO Nanocomposites

The formed Ag/ZnO nanocomposite will be dispersed into distilled water and analyzed using a UV-Vis spectrophotometer for 6 days to determine the stability of the Ag/ZnO nanocomposite that has been made. The measurement results can be seen in Figure 3 and Table 2.

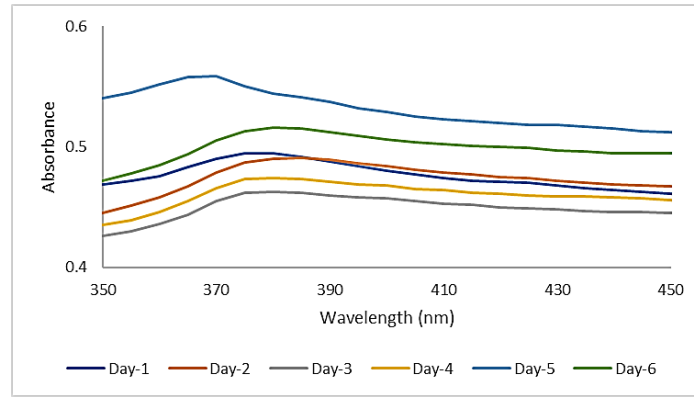


Figure 3. Results of Ag/ZnO Nanocomposite Analysis Using UV-Vis Spectrophotometer

Based on Figure 3 and Table 2, the Ag/ZnO is characteristic of ZnO. During the 6 days, no new nanocomposite tends to be stable for 6 days. The peaks appeared and the absorbance did not decrease drastically. The peak formed at a wavelength of 370–385 nm, which

Table 2. UV-Vis Spectrophotometer Data of Ag/ZnO Nanocomposites Over 6 Days

Day	λ_{max} (nm)	Absorbance
1	380	0,495
2	385	0,491
3	380	0,463
4	380	0,474
5	370	0,559
6	380	0,516

On the 5th day, the absorbance increased, presumably due to the sample being less homogeneous before analysis. In the Ag/ZnO nanocomposite, the absorption peak from silver nanoparticles is not visible, presumably due to the smaller number of silver nanoparticles and the dispersion of silver nanoparticles on the ZnO surface.

Characterization of Ag/ZnO Nanocomposites with PSA

The formed Ag/ZnO nanocomposites will be characterized using a Particle Size Analyzer (PSA) to determine the particle size distribution in the Ag/ZnO nanocomposites, as shown in Figure 4.

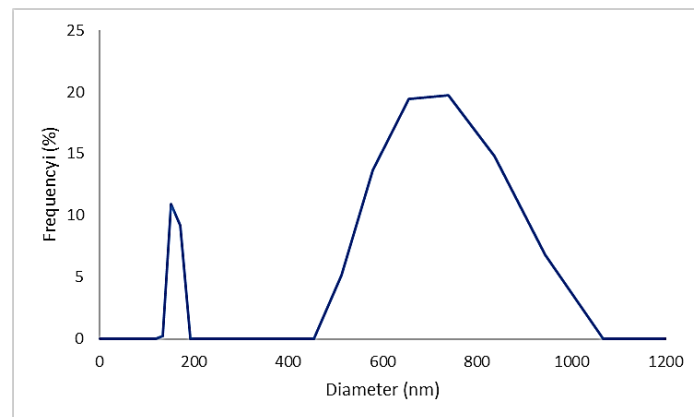


Figure 4. Characterization Results of Ag/ZnO Nanocomposites Using a Particle Size Analyzer (PSA)

The method used for characterizing the Particle Size Analyzer (PSA) is Dynamic Light Scattering (DLS). The particle size distribution is bimodal, with dominant sizes at 150.8 nm and 671.2 nm. A Polydispersity Index (PI) value of 0.490 indicates a polydisperse condition tending toward aggregation. The Z-average value of 1009.1 nm confirms the presence of agglomeration in the suspension, indicating that the system has not yet achieved optimal colloidal stability. A PDI value >0.1 indicates an increasingly non-homogeneous particle distribution. In DLS measurements, agglomerated

particles cannot be measured individually, so their hydrodynamic size is often much larger than the primary particle size observed using TEM [23].

Characterization of Ag/ZnO Nanocomposites with TEM

The formed Ag/ZnO nanocomposites will be characterized using Transmission Electron Microscopy (TEM) to determine the morphology, structure, and size of the particles. The morphology of the formed Ag/ZnO nanocomposites can be seen in Figure 5.

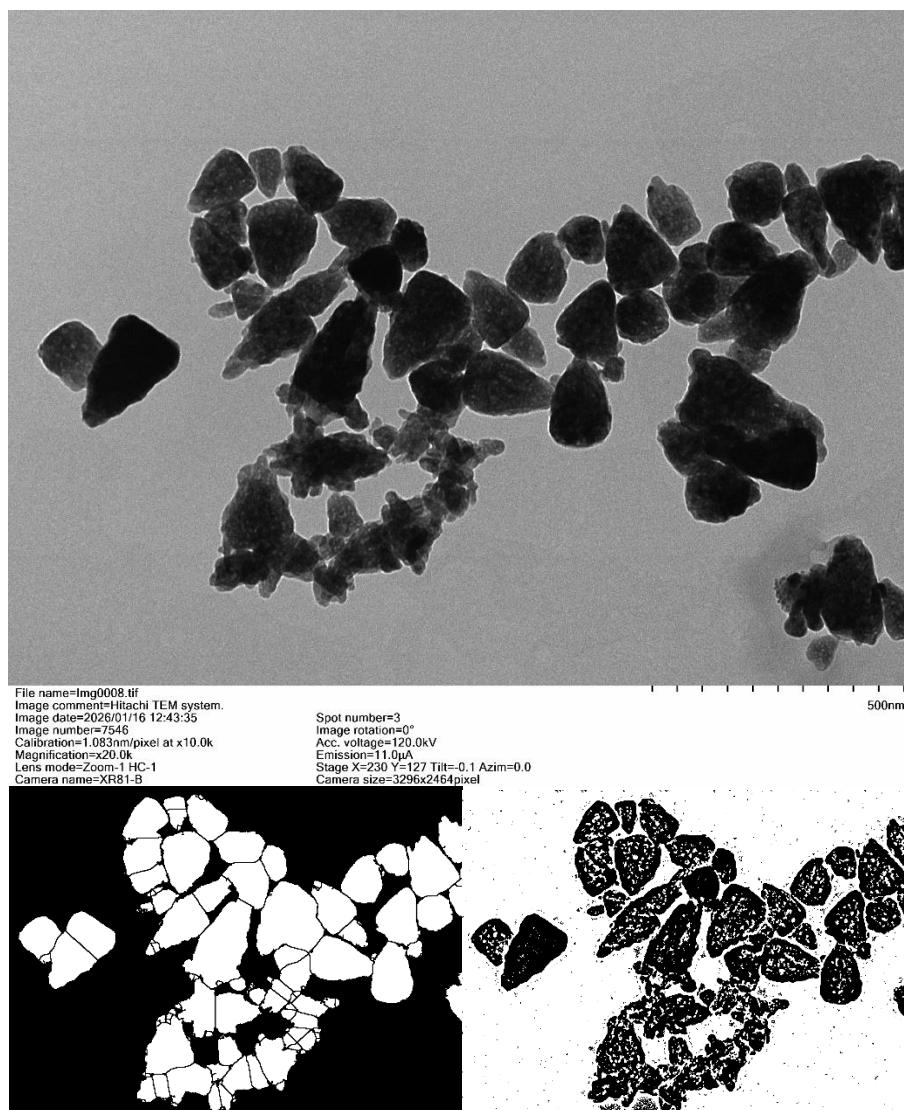


Figure 5. Characterization Results of Ag/ZnO Nanocomposites using Transmission Electron Microscopy (TEM)

Based on Figure 5, it can be seen that the morphology of ZnO as a matrix is blunt triangular and tends to be less uniform with irregular silver nanoparticles that tend to agglomerate distributed on the surface of ZnO. This also supports the results of the UV-Vis

Spectrophotometer where the absorption peak of silver nanoparticles is not visible. After that, the particle size distribution was determined using Image J software, as shown in Figures 6 and 7.

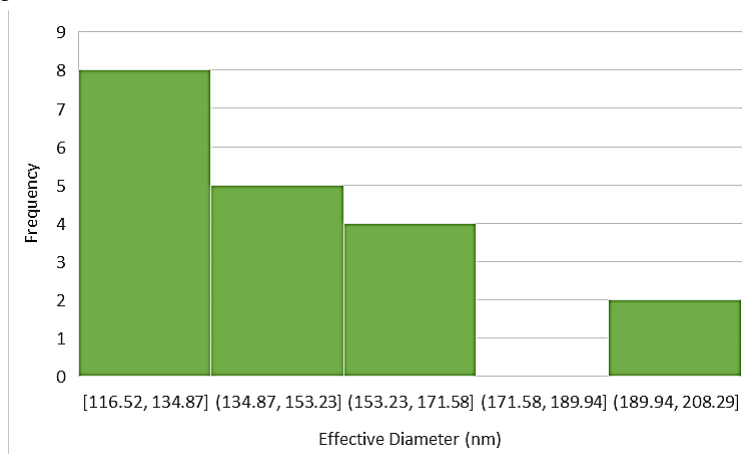


Figure 6. Histogram of ZnO Size Distribution Based on Image J Software

The majority of ZnO particle size distribution is in the range of 116.52–134.87 nm. The average effective diameter \pm standard deviation of ZnO is

145.45 ± 25.95 . This value is not far from the PSA value obtained, which is 150.8 nm.

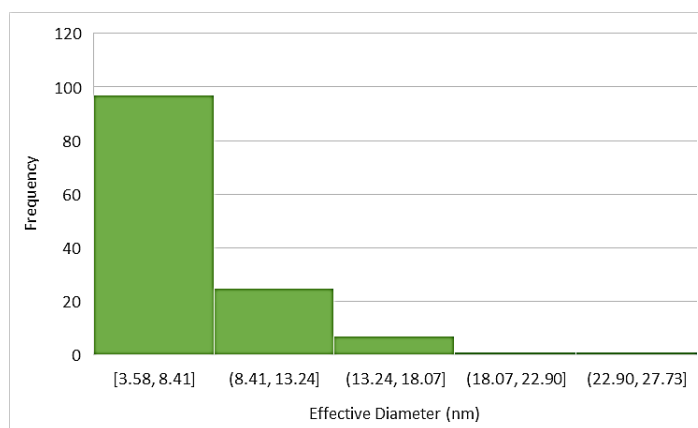


Figure 7. Histogram of AgNP Size Distribution Based on Image J Software

The majority of silver nanoparticle size distribution is in the range of 3.58–8.41 nm. The average effective diameter \pm standard deviation of silver nanoparticles is 7.25 ± 3.73 .

Characterization of Ag/ZnO Nanocomposites with XRD

The formed Ag/ZnO nanocomposites will be characterized using X-Ray Diffraction (XRD) to determine the structure and crystal phase of the Ag/ZnO nanocomposites, as shown in Figure 8.

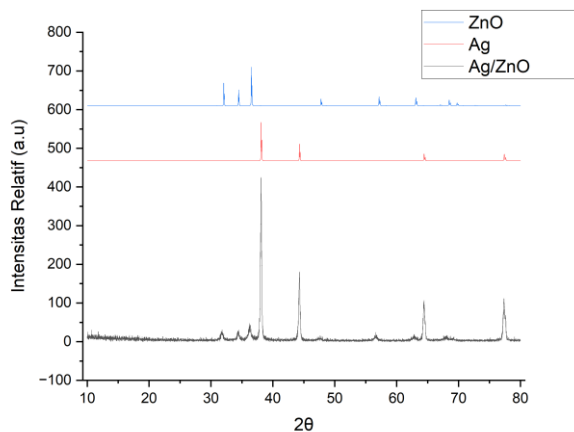


Figure 8. Characterization Results of Ag/ZnO Nanocomposites using X-Ray Diffraction (XRD)

Based on Figure 8, the Ag/ZnO nanocomposite exhibits strong and sharp XRD peak intensities, indicating a high degree of crystallinity. The XRD pattern of the Ag/ZnO nanocomposite displays diffraction peaks around 31.7, 34.4, 36.2, 47.5, 56.6, 62.8, and 66–68, which are indexed to the crystal planes (100), (002), (101), (102), (110), (103), and (200)/(112) planes, corresponding to the hexagonal wurtzite structure of ZnO according to the JCPDS standard (PDF 36-1451). The characteristic peaks of ZnO did not shift significantly, suggesting that the ZnO crystal structure is stable. In addition, the peaks at 38.1, 44.3, 64.4, and 77.4 are indexed to the crystal planes (111), (200), (220) and (311) in the form of a face-centered cubic (FCC) Ag structure in accordance with the JCPDS 04-0783 standard. The dominant intensities between the two phases are around 36 for ZnO (101) and 38 for Ag (111), which means that ZnO is the main matrix and Ag is dispersed as nanoparticles on the ZnO surface.

CONCLUSION

Ag/ZnO nanocomposites were successfully synthesized with the following characteristics formed at λ_{\max} (nm) 370–385 nm and stable for 6 days. The particle size distribution is bimodal, with dominant sizes at 150.8 nm and 671.2 nm. The morphology of ZnO as a matrix is blunt triangular and tends to be less uniform with irregular silver nanoparticles that tend to agglomerate and are scattered on the ZnO surface. Based on the results of

the image J software, most of the ZnO particle size distribution was in the range of 116.52–134.87 nm. The average effective diameter \pm standard deviation of ZnO was 145.45 ± 25.95 , and most of the silver nanoparticle size distribution was in the range of 3.58–8.41 nm. The average effective diameter \pm standard deviation of silver nanoparticles is 7.25 ± 3.73 . ZnO has a hexagonal wurtzite structure and Ag has a face-centered cubic (FCC) structure, so ZnO becomes the main matrix and Ag is dispersed as nanoparticles on the surface of ZnO.

REFERENCES

- A. Baig, M. Siddique, and S. Panchal, “A Review of Visible-Light-Active Zinc Oxide Photocatalysts for Environmental Application,” Feb. 01, 2025, Multidisciplinary Digital Publishing Institute (MDPI). doi: 10.3390/catal15020100.
- A. Nafiisah, R. Purnamasari, and S. Mudalianah, “Identifikasi Senyawa Metabolit Sekunder pada Ekstrak Etanol Daun Binahong,” *Jurnal Sosial Dan Sains*, vol. 4, no. 11, pp. 1093–1106, 2024, [Online]. Available: <http://sosains.greenvest.co.id>
- A. Nafis, D. Septiani, and J. Malau, “Antibacterial activity test of ceremai leaf extract (*Phyllanthus acidus* (L.) Skeels) against *Staphylococcus aureus*,” *Journal of*

- Pharmaceutical and Sciences, vol. 6, no. 3, pp. 1194–1203, 2023.
- A. R. Z. Zam, N. Amin, and S. Redjeki, “Sintesis dan Karakterisasi Nanopartikel Perak Berbasis AgNO₃ dan Ekstrak Daun Lamtoro (*Leucaena Leucocephala*) untuk Aktivitas Antibakteri,” *Serambi Engineering*, vol. XI, no. 1, pp. 16532–16543, Jan. 2026.
- A. S. Rini, A. P. Defiti, R. Dewi, Jasril, and Y. Rati, “Biosynthesis of nanoflower Ag-doped ZnO and its application as photocatalyst for Methylene blue degradation,” in *Materials Today: Proceedings*, Elsevier Ltd, 2023, pp. 234–239. doi: 10.1016/j.matpr.2023.03.100.
- A. S. Zulaicha et al., “Green Synthesis Nanopartikel Perak (AgNPs) Menggunakan Bioreduktor Alami Ekstrak Daun Ilalang (*Imperata cylindrica* L),” 2021.
- F. A. Saputra, I. W. Karyasa, and G. A. B. Widana, “Green Synthesis dan Karakterisasi Nanopartikel Tembaga Oksida Dari Tembaga(II) Asetat Menggunakan Ekstrak Rimpang Kunyit (*Curcuma longa* L.),” 2024.
- F. Mita, A. Jumarni, R. Wati, A. Patimah, and D. Y. Rahman, “Perkembangan Penerapan Nanoteknologi di Bidang Pelapisan (Coating),” *Jurnal Penelitian Fisika dan Terapannya (Jupiter)*, vol. 5, no. 2, pp. 1–29, 2024, doi: 10.31851/jupiter.v5i2.33738.
- J. G. Cuadra et al., “ZnO/Ag Nanocomposites with Enhanced Antimicrobial Activity,” *Applied Sciences (Switzerland)*, vol. 12, no. 10, pp. 1–13, May 2022, doi: 10.3390/app12105023.
- J. K. Marpaung, Suharyanisa, M. Situmorang, and A. Loi, “Identifikasi Simplisia Dan Uji Aktivitas Aantibakteri Daun Ceremai (*Phyllanthus acidus* (L.) Skeels) Terhadap Bakteri *Streptococcus pyogenes* Dan Bakteri *Salmonella typhi*,” *Jurnal TEKESNOS*, vol. 4, no. 1, pp. 307–318, May 2022.
- J. R. L. López et al., “*Tagetes erecta*—Mediated Green Synthesis of ZnO–Ag Nanocomposites: Characterization and Dual Applications in Solar Photocatalytic Degradation and Antibacterial Activity,” *Ceramics*, vol. 8, no. 2, pp. 1–23, Jun. 2025, doi: 10.3390/ceramics8020045.
- Lelawati, E. Tonadi, and Aan Sefentry, “Analisis Kekerasan Papan Komposit dari Serat Pelepah Pisang Dengan Resin Polyester,” *Jurnal Redoks*, vol. 8, no. 2, pp. 152–157, Dec. 2023, doi: 10.31851/redoks.v8i2.13614.
- M. S. A. Galil, M. Al-qubati, S. O. Mohammed, A. Numan, A. A. R. Saeed, and E. A. A. Saif, “Effect of single and combined (core/shell) biosynthesis of nanoparticles (Ag and ZnO) on their photocatalytic and antimicrobial activities,” *Kuwait Journal of Science*, vol. 52, no. 2, pp. 1–15, Apr. 2025, doi: 10.1016/j.kjs.2024.100356.
- N. Fajri, L. F. A. Putri, M. R. Prasetio, N. Azizah, Y. Pratama, and N. C. A. Susanto, “Potensi Batang Pisang (*Musa paradisiaca* l) sebagai bioreduktor dalam Green Sintesis Ag nanopartikel,” *Jurnal Penelitian Sains*, vol. 24, no. 1, pp. 33–37, May 2022, doi: 10.56064/jps.v24i1.668.
- N. Handayani, “NANOKOMPOSIT RAMAH LINGKUNGAN MELALUI ISOLASI NANOFIBRIL SELULOSA (NFS) DARI TANDAN KOSONG SAWIT DAN POLY LACTID ACID (PLA) SEBAGAI MATRIK,” Dec. 2020.
- R. A. Sephia, M. O. Rahayu, N. R. Adawiyah, D. N. Fatwa, and I. L. P. Mursal, “Review Artikel : Analisis Karakteristik Dan

- Pengaplikasian Teknologi Nanopartikel Berdasarkan Klasifikasinya Pada Berbagai Jenis Terapi,” *Jurnal Ilmiah Wahana Pendidikan*, vol. 9, no. 18, pp. 675–682, 2023, doi: 10.5281/zenodo.8324839.
- R. F. Fard, R. Aali, S. M. Aghdam, and S. Mortazaviderazkola, “The surface modification of spherical ZnO with Ag nanoparticles: A novel agent, biogenic synthesis, catalytic and antibacterial activities,” *Arabian Journal of Chemistry*, vol. 15, no. 3, pp. 1–15, Mar. 2022, doi: 10.1016/j.arabjc.2021.103658.
- S. B. Waruwu, A. P. Sari, D. Satria, E. D. L. Putra, P. A. Z. Hasibuan, and Y. M. Choo, “Utilization of *Artocarpus altilis* leaf extract for silver nanoparticle synthesis: Comparative antioxidant and antibacterial evaluation with water extract,” *S. Afr. J. Chem. Eng.*, vol. 53, pp. 516–526, Jul. 2025, doi: 10.1016/j.sajce.2025.06.013.
- S. K. Filippov et al., “Dynamic light scattering and transmission electron microscopy in drug delivery: a roadmap for correct characterization of nanoparticles and interpretation of results,” Sep. 26, 2023, Royal Society of Chemistry. doi: 10.1039/d3mh00717k.
- S. Shanmugam K, L. Ramkumar, R. Jagadeesan, M. Maghimaa, N. Hemapriya, and . Suresh S, “Green synthesis of bimetallic Ag-ZnO nanocomposite using polyherbal extract for antibacterial and anti-inflammatory activity,” *Chemical Physics Impact*, vol. 9, pp. 1–7, Dec. 2024, doi: 10.1016/j.chphi.2024.100763.
- S. Sijabat and H. Dabbuke, “SOSIALISASI DAN SIMULASI TIMBANGAN PADA HOTPLATE MAGNETIC STIRRER BERBASIS ARDUINO UNO,” *Jurnal Pengabdian Masyarakat Universitas Sari Mutiara Indonesia*, vol. 03, no. 1, pp. 536–541, Feb. 2022.
- V. Amrute, Monika, K. K. Supin, M. Vasundhara, and A. Chanda, “Observation of excellent photocatalytic and antibacterial activity of Ag doped ZnO nanoparticles,” *RSC Adv.*, vol. 14, no. 45, pp. 32786–32801, 2024, doi: 10.1039/D4RA05197A.
- Z. Liang et al., “Enhancement of photocatalytic and antibacterial activities of zinc oxide nanoparticles through in-situ loading of well-dispersed silver nanoparticles,” *Inorg. Chem. Commun.*, vol. 177, p. 114414, Jul. 2025, doi: 10.1016/j.inoche.2025.114414.